Strong Laser Field Induced Modifications of Electron-Transfer Processes in Ne^+–He Collisions

Z.Z. Lu*, Y.L. Sun, L. Ma and J.F. Liu
School of Physics and Optoelectronic Engineering, Xidian University, Xi'an 710071, China

(Received September 21, 2016; in final form March 30, 2017)

A strong laser field ($\approx 10^{15}$ W/cm^2) induced low-collisional-energy charge transfer process in Ne^+–He system is explored. In the low collisional energy regime, the cross-section can be $\approx 10^{-17}$ cm^2 which is about two orders of magnitude higher than the collision-only process. With increasing collisional energy the cross-section curve displays flattens and the charge capture tends to be practically independent of the laser detuning. In addition, we find that the capture probability in this Ne^+–He system varies significantly with the laser polarization angle.

DOI: 10.12693/APhysPolA.131.1519
PACS/topics: 32.70.Jz, 34.50.–s

1. Introduction

Ion-atom charge-transfer process is of considerable interest both from a fundamental and from a more applied point of view in the areas of laser physics and fusion research. It might broaden and deepen our general understanding of dynamic atomic processes, and it makes significant steps to detailed understanding of active control of atomic dynamics. However, in the low-energy collision region, the energy defect of the donor (atom) and the acceptor (ion) severely suppresses the charge-transfer cross-section. There is interest in using a laser to overcome the energy defect factor and the charge transfer cross-section can be greatly increased by several orders by the joint action of the collisional and radiative interactions [1].

In the early work, most attention was focused on the laser frequency resonant effects and the researches were performed for relatively low intensities ($< 10^{10}$ W/cm^2) [2–9]. In more recent works, people have focused on laser intensities above 10^{13} W/cm^2 and many theoretical models have been proposed [10–14].

In the present work, we discuss a strong laser field ($\approx 10^{15}$ W/cm^2) induced low-collisional-energy charge transfer process. The strong laser field enhanced charge-transfer collision between Ne^+ and He atom can be described by the following expression:

$$Ne^+ + He(1s^2\ ^1S_0) + \hbar\omega \rightarrow Ne(2p^6\ ^1S_0) + He^+$$

We prefer to observe the significant modifications of collisional processes when both types of collision and laser field interactions are combined. Since the laser intensity is $\approx 10^{15}$ W/cm^2, the role of the applied laser field will be different from the one in the early work.

Considering the reaction $Ne^+ + He \rightarrow Ne + He^+$ from the point of the gases ionizing potential, since the ionization potentials of the Ne and He are 21.6 V and 24.6 V, respectively, it will be seen that in the absence of the laser field and at very low impact velocity, the charge transfer is most probable in the case of $Ne^+ + He \rightarrow Ne^+ + He^+$, which is a reverse reaction of $Ne^+ + He \rightarrow Ne + He^+$ and has been studied by Harnwell [15]. This argument as given is not strictly applicable to the present conditions, because the present reaction combines collision with an external strong field with the laser field intensity of $\approx 10^{15}$ W/cm^2. When the dipole interaction $-\boldsymbol{E}\cdot\boldsymbol{d}$ is added to the molecular potentials, the initial and final states potentials will cross and charge exchange from He atom to Ne^+ occurs at the crossing [16, 17]. Therefore the reaction $Ne^+ + He \rightarrow Ne + He^+$ needs the participation of strong laser field and it will be enhanced obvious.

2. The theoretical model

The laser induced charge transfer (LICT) process between ion A^+ and atom B can be described by a three-body system as shown in Fig. 1, and also can be described by the following expression:

$$A^+ + B + \hbar\omega \rightarrow A + B^+.$$

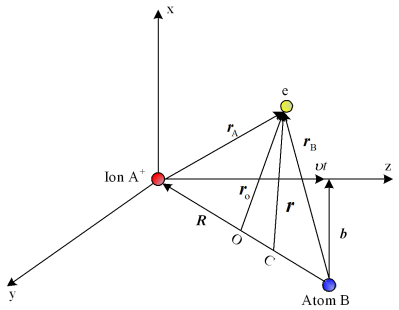

Fig. 1. Schematic diagram of the three-body system for laser induced charge transfer.

During the collision process between ion A^+ and atom B, because of the simultaneous effects of both collision and the strong laser field, an outer-shell electron e of

*corresponding author; e-mail: luhit@126.com

atom B is transferred to A^+. At the same time the atom B is ionized, and ion A^+ transits to its atomic ground state.

In Fig. 1, electron e denotes the bound electron of atom B; $\boldsymbol{R}(t)$ is the position vector between the two ion cores. $\boldsymbol{r}_{\rm A}$ and $\boldsymbol{r}_{\rm B}$ are the position vectors of electrons e with respect to the ion cores, respectively; $\boldsymbol{r}$ is the position vector of electron e with respect to the centroid C; $\boldsymbol{r}_O$ is the position vector of electrons e with respect to the centre of the two ion cores O. Therefore, the time-dependent Schrödinger equation in the centre of mass coordinate system for the whole system is

$$\mathrm{i}\hbar\frac{\partial\phi}{\partial t} = (T+V)\,\phi, \tag{1}$$

where ϕ is the total wave function of the system, T and V are the kinetic energy and potential energy operators, respectively.

The kinetic energy and potential energy operators of the three-body system can be expressed as

$$T = -\frac{\hbar^2}{2\mu}\nabla_R^2, \tag{2}$$

$$V = V_{\rm A^+B^+} + V_{\rm A^+e} + V_{\rm B^+e} + V_f + V_e \tag{3}$$

where μ_e and μ are the reduced masses of the two electrons and the two ion cores, respectively. V_f is the interaction between the laser field and the colliding particles. V_e is the interaction between the laser field and electron.

$$V_{\rm A^+B^+} = \frac{e^2}{4\pi\varepsilon_0 R}, \tag{4}$$

$$V_{\rm A^+e} = -\frac{e^2}{4\pi\varepsilon_0 r_{\rm A}}, \tag{5}$$

$$V_{\rm B^+e} = -\frac{e^2}{4\pi\varepsilon_0 r_{\rm B}}, \tag{6}$$

$$V_{\rm e}(t) = \boldsymbol{A}(t)\cdot(-\mathrm{i}\boldsymbol{\nabla}) + \frac{A^2(t)}{2}, \tag{7}$$

where

$$\boldsymbol{A}(t) = -\int_{-\infty}^{t}\boldsymbol{E}(\tau)\,\mathrm{d}\tau, \tag{8}$$

$$V_f = \boldsymbol{f}_{\rm AB}(\boldsymbol{r}_{\rm A},\boldsymbol{r}_{\rm B},\boldsymbol{R}(t))\cdot\boldsymbol{E}(t), \tag{9}$$

where

$$\boldsymbol{f}_{\rm AB} = -e(\frac{\boldsymbol{r}_{\rm A}+\boldsymbol{r}_{\rm B}}{2}) + \frac{1}{2}e(p-q)\boldsymbol{R}(t), \tag{10}$$

$$q = M_{\rm A}/(M_{\rm A}+M_{\rm B}), \tag{11}$$

$$p = M_{\rm B}/(M_{\rm A}+M_{\rm B}), \tag{12}$$

$$R = (b^2+\upsilon^2t^2)^{1/2}, \tag{13}$$

$$\boldsymbol{E}(t) = \boldsymbol{\varepsilon}\cdot E_0 f(t)\cos\omega t. \tag{14}$$

In Eq. (11) and Eq. (12), the M_A and $M_{\rm B}$ are the masses of ion A and B, respectively. In Eq. (14) $\boldsymbol{E}(t)$ is the laser field, where $\boldsymbol{\varepsilon}$ is the unit vector of polarization direction, E_0 is the amplitude of the field intensity, $f(t)$ is the pulse envelope and can be expressed as

$$f(t) = \exp(-t^2/\sigma^2) \tag{15}$$

where

$$\sigma \cong \frac{3\tau}{5}, \tag{16}$$

with τ being the pulse width.

The motion of the two ion cores can be described by wave function $F(\boldsymbol{R})$ which meets the following scattering equation:

$$\left(-\frac{\hbar^2}{2\mu}\nabla_R^2 - \bar{E}\right)F(\boldsymbol{R}) = 0, \tag{17}$$

where $\bar{E}$ is the energy of the system.

Then the total wave function of the system, i.e. $\phi(R,r)$, can be written as the product of $F(\boldsymbol{R})$ and the wave function of the electron

$$\phi(\boldsymbol{R},\boldsymbol{r}) = F(\boldsymbol{R})\psi(\boldsymbol{R},\boldsymbol{r}). \tag{18}$$

Substituting Eq. (18) into Eq. (1), we can obtain

$$-\frac{\hbar^2}{2\mu}F(\boldsymbol{R})\nabla_R^2\psi(\boldsymbol{R},\boldsymbol{r}) - \frac{\hbar^2}{\mu}\nabla_R F(\boldsymbol{R})\cdot\nabla_R\psi(\boldsymbol{R},\boldsymbol{r}) + F(\boldsymbol{R})H_e\psi(\boldsymbol{R},\boldsymbol{r}) = 0, \tag{19}$$

where

$$H_e = -\frac{\hbar^2}{2\mu_e}\nabla_r^2 + V. \tag{20}$$

The first two terms in Eq. (19) describe the coupling of motions of the ion cores and the electrons. For a classical straight-line trajectory in which the relative velocity υ is parallel to the z axis, $F(\boldsymbol{R})$ is a plane wave in the form

$$F(\boldsymbol{R}) = \exp(\mathrm{i}\frac{\mu}{\hbar}\upsilon\cdot z_R), \tag{21}$$

where $z_R = \upsilon t$.

Substituting Eq. (21) into Eq. (19), the first term can be omitted because the reduced mass μ is a large parameter; Eq. (19) can be rewritten as

$$H_e\psi(\boldsymbol{R},\boldsymbol{r}) = \mathrm{i}\hbar\upsilon\frac{\partial}{\partial z_R}\psi(\boldsymbol{R},\boldsymbol{r}). \tag{22}$$

Then Eq. (22) can be rewritten as a time-dependent Schrödinger equation as follows:

$$H_e\psi(\boldsymbol{r},t) = \mathrm{i}\hbar\frac{\partial}{\partial t}\psi(\boldsymbol{r},t), \tag{23}$$

where $\psi(\boldsymbol{r},t)$ is the wave function of the electron.

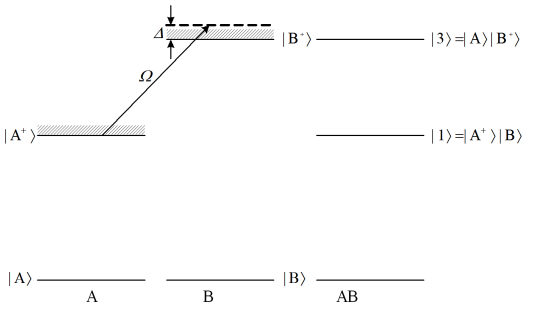

Fig. 2. Energy levels of laser induced charge transfer.

For the three-level system of laser-induced collisional energy transfer between ion A^+ and atom B shown in Fig. 2, the following two levels of the compound system can be formed by the energy levels of ion A^+ and B^+ as follows:

$$|1\rangle = |\mathrm{A}^+\rangle|\mathrm{B}\rangle, \tag{24}$$

$$|3\rangle = |\mathrm{A}\rangle|\mathrm{B}^+\rangle. \tag{25}$$

The compound state $|1\rangle$ is the initial state of the laser induced charge transfer process, and the $|3\rangle$ is the final state

$$\varphi_1(\boldsymbol{r},t) = \phi_1(\boldsymbol{r}_\mathrm{B})\exp(\mathrm{i}\alpha_1), \tag{26}$$

$$\varphi_3(\boldsymbol{r},t) = \phi_3(\boldsymbol{r}_\mathrm{A})\exp(\mathrm{i}\alpha_2), \tag{27}$$

where

$$\alpha_1 = -\frac{\eta_1}{\hbar}t - \frac{\mu_e}{\hbar}q\boldsymbol{v}\cdot\boldsymbol{r} - \frac{\mu_e}{2\hbar}q^2v^2t, \tag{28}$$

$$\alpha_2 = -\frac{\eta_2}{\hbar}t + \frac{\mu_e}{\hbar}p\boldsymbol{v}\cdot\boldsymbol{r} - \frac{\mu_e}{2\hbar}p^2v^2t, \tag{29}$$

with η_1 and η_2 being eigenvalues of $\phi_1(\boldsymbol{r}_\mathrm{B})$ and $\phi_3(\boldsymbol{r}_\mathrm{A})$, respectively.

In addition to the initial state and the final state, the contribution of an important intermediate state $\varphi_2(r,t)$ to the charge transfer process is considered. $\varphi_2(r,t)$ is the wave function of the electron in a state excited to the continuum. Since the Volkov solutions are eigenfunctions of the $V_e(t)$ operator for free electrons in the presence of laser field, we express the wave function of the active electron as

$$\varphi_2(r,t) = \frac{1}{(2\pi)^{3/2}}\exp\Big(\mathrm{i}\boldsymbol{p}\cdot\boldsymbol{r} - \frac{\mathrm{i}p^2t}{2} - \mathrm{i}\int_{-\infty}^{t}\mathrm{d}\tau\left(\boldsymbol{A}(\tau)\cdot\boldsymbol{p} + A^2(\tau)/2\right)\Big). \tag{30}$$

For the monochromatic polarized laser field, $\varphi_2(r,t)$ can be given by

$$\varphi_2(\boldsymbol{r},t) = 1/(2\pi)^{3/2}\exp\big(\mathrm{i}\left(\boldsymbol{p}\cdot\boldsymbol{r} - p^2t/2 - U_pt + \xi\sin\omega t - (U_p/2\omega)\sin 2\omega t\right)\big), \tag{31}$$

where, is the ponderomotive potential, and $\boldsymbol{p}$ denotes the momentum of the active electron in the continuum state.

Expanding the wave function of the electrons using the primary functions expressed by formulae (26), (27), and (31):

$$\psi(\boldsymbol{r},t) = \sum_n c_n\varphi_n \ (n=1,2,3). \tag{32}$$

Using the interaction Hamiltonian in formula (20) and the primary functions expressed by formulae (26), (27), and (31), we can derive the equations of motion for the probability amplitudes

$$\mathrm{i}\hbar\left(\dot{c}_1 + S_{12}\dot{c}_2 + S_{13}\dot{c}_3\right) = H_{11}c_1 + H_{12}c_2 + H_{13}c_3, \tag{33}$$

$$\mathrm{i}\hbar\left(S_{12}^*\dot{c}_1 + \dot{c}_2 + S_{23}\dot{c}_3\right) = H_{21}c_1 + H_{22}c_2 + H_{23}c_3 \tag{34}$$

$$\mathrm{i}\hbar\left(S_{13}^*\dot{c}_1 + S_{32}\dot{c}_2 + \dot{c}_3\right) = H_{31}c_1 + H_{32}c_2 + H_{33}c_3 \tag{35}$$

where

$$S_{mj} = \int\varphi_m^*\varphi_j\,\mathrm{d}^3\tau,$$

$$H_{mn} = \int\varphi_m^*\left(H_e - i\hbar\frac{\partial}{\partial t}\right)\varphi_n\,\mathrm{d}^3\tau$$

Taking a unitary transformation of matrix the equation of motion for the probability amplitudes can be simplified as

$$\mathrm{i}\hbar\begin{bmatrix}\dot{c}_1\\ \dot{c}_2\\ \dot{c}_3\end{bmatrix} = \begin{bmatrix}A_{11} & A_{12} & A_{13}\\ A_{21} & A_{22} & A_{23}\\ A_{31} & A_{32} & A_{33}\end{bmatrix}\begin{bmatrix}c_1\\ c_2\\ c_3\end{bmatrix}, \tag{36}$$

where

$$A_{11} = \frac{H_{11} - H_{21}S_{12}}{1-|S_{12}|^2}, \tag{37}$$

$$A_{12} = \frac{H_{12} - H_{22}S_{12}}{1-|S_{12}|^2}, \tag{38}$$

$$A_{13} = \frac{H_{13} - H_{23}S_{12}}{1-|S_{12}|^2,} \tag{39}$$

$$A_{21} = \frac{H_{21} - H_{31}S_{23}}{1-|S_{23}|^2}, \tag{40}$$

$$A_{22} = \frac{H_{22} - H_{32}S_{23}}{1-|S_{23}|^2}, \tag{41}$$

$$A_{23} = \frac{H_{23} - H_{33}S_{23}}{1-|S_{23}|^2}, \tag{42}$$

$$A_{31} = \frac{H_{31} - H_{11}S_{31}}{1-|S_{13}|^2}, \tag{43}$$

$$A_{32} = \frac{H_{32} - H_{12}S_{31}}{1-|S_{13}|^2}, \tag{44}$$

$$A_{33} = \frac{H_{33} - H_{13}S_{31}}{1-|S_{13}|^2}, \tag{45}$$

Equation (36) meets the initial conditions that

$$\begin{cases}|c_1(-\infty)|^2 = 1\\ |c_2(-\infty)|^2 = 0\\ |c_3(-\infty)|^2 = 0\end{cases}. \tag{46}$$

Then the expression of the collision cross-section can be obtained

$$\sigma = 2\pi\int_0^\infty b\cdot|c_2(b,+\infty)|^2\,\mathrm{d}b. \tag{47}$$

3. Results and discussions

During the collision process between Ne^+ and He atom, because of the simultaneous effects of both collision and the strong laser field, the energy of Ne^+ is transferred to atom He which at the same time is ionized because of loss of an outer-shell electron, while Ne^+ transits to its atomic ground state. The process also can be described by the following expression:

$$\mathrm{Ne}^+ + \mathrm{He}(1s^2\ {}^1S_0) + \hbar\omega \rightarrow \mathrm{Ne}(2p^6\ {}^1S_0) + \mathrm{He}^+. \tag{48}$$

The charge-transfer cross-section as a function of impact energy for the Ne^+–He system at different transfer laser wavelength is shown in Fig. 3.

In the low-collisional energy region ($E_p < 4\times10^{-4}$ keV/amu), the collisional coupling is relatively weak while the laser coupling plays a dominant role. When

the laser field added to the collisional system, the cross-section is inversely proportional to the collisional energy as indicated by the Landau–Zener formula [1]. We observe a strong propensity for an enhancement of the charge transfer cross-section. For a collision-only process, the charge transfer cross-section is $\approx 10^{-19}$ cm^2, and in the combination of both laser and collision, the cross-section can be $\approx 10^{-17}$ cm^2 which is about two orders of magnitude higher than the collision-only process.

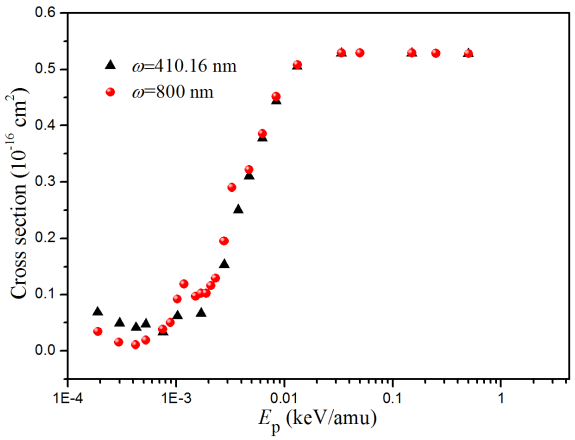

Fig. 3. Charge-transfer cross-section as a function of impact energy for Ne^+–He system at different transfer laser wavelength.

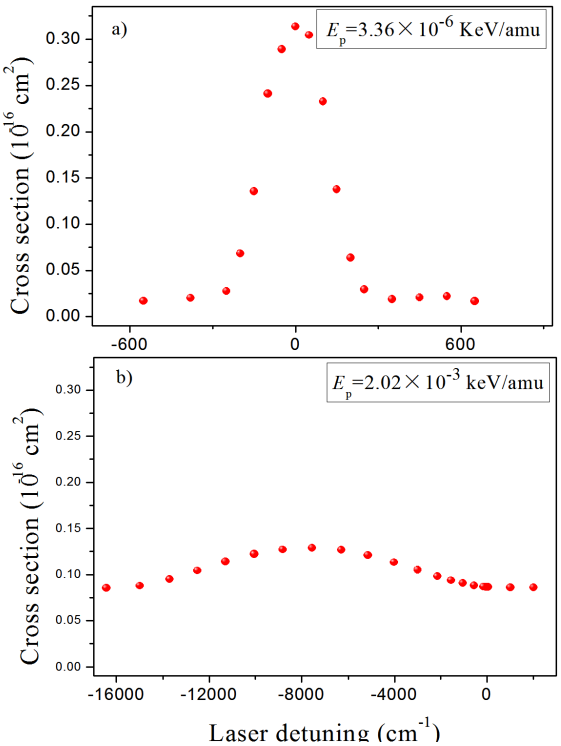

Fig. 4. Charge-transfer cross-section as a function of laser detuning at different impact energy for Ne^+–He system.

With the increase of the collisional energy ($E_p > 1.13 \times 10^{-2}$ keV/amu), the collisional coupling tends to play a dominant role and the charge transfer cross-section for the Ne^+–He system in the presence and absence of a laser field tends to be equal. Moreover, the two kinds of couplings are of equal importance only in the region from 4×10^{-4} keV/amu to 1.13×10^{-2} keV/amu, where the interference between these two coupling is evident.

In the collisional energy range from 1×10^{-4} keV/amu to 1×10^{-3} keV/amu, although the non-resonant transition ($\omega = 800$ nm) matrix element is far less than the resonant transition ($\omega = 410.16$ nm), the charge transfer cross-sections of non-resonant transition and resonant transition are in the same order of magnitude. Such results indicate that even though the laser detuning is relatively large, we still can realize the interparticle charge transfer.

When the transfer laser field intensity is 1×10^{15} W/cm^2, the laser detuning dependence of the field-assisted collisional charge transfer cross-section is studied in Fig. 4.

In weak field, the results are characterized by a universal profile with the full width at half peak of the profile being $\approx 2 \times 10^2$ cm^{-1}, which is wider in an order of magnitude than the results of laser-induced energy transfer processes characterized by the full width at half peak of the profile being less than 10 cm^{-1}. The strongest enhancement is found around $\Delta = 0$ cm^{-1} for the low-collisional energy indicating that the laser induced charge transfer is most effective in this region, which is based on the fact that interparticle transition takes place only in the neighborhood of the resonance points and a qualitatively similar behavior was observed in an early study of laser-assisted capture in He^{2+}–H collisions [18].

With increase of collisional energy ($E_p = 2.02 \times 10^{-3}$ keV/amu) the cross-section curve displayed in Fig. 4b flattens and the charge capture tended to be practically independent of the laser detuning. The peak of the cross-section profile is not found when the transfer laser is strictly resonant, but it is found when the transfer laser detunes from $\Delta = -7750$ cm^{-1}. Moreover, the FWHM increases to 8922 cm^{-1}. It is in this collisional energy region that the projectile potential is strong enough to induce appreciable electronic transitions.

When the laser is polarized perpendicular to the projectile trajectory, one more parameter appears: the angle between the laser polarization and the collision plane.

In our previous experiment work [19], we observed that the capture probability in laser-induced Ne^+–He collision varied significantly with the laser polarization angle, i.e. the signal of He^+ strongly depends on the laser polarization. For the horizontal polarization, a maximum was observed, but the signal was much smaller when the polarization was nearly perpendicular. Comparing with the case of $\alpha = \frac{\pi}{2}$, for polarization in the horizontal plane ($\alpha = 0$), the signal intensity was about a 32.9% increase. In contrast, the calculation result of the strong variation of the charge transfer cross-section is evident from Fig. 5.

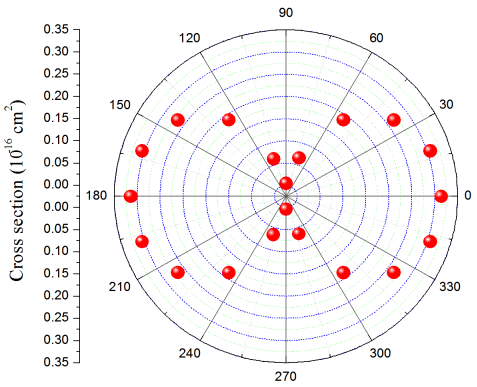

Fig. 5. Charge-transfer cross-section as a function of the angle between the laser polarization and the collision plane for Ne^+–He system.

The capture probability in laser-assisted atom–ion collision varies significantly with the laser polarization angle. For the horizontal polarization, we observe a maximum, but the cross-section is much smaller when the polarization is nearly perpendicular. The observed anisotropy of the cross-section angular distribution is in coincidence with previous experiment results [19]. Such an interesting feature of the relative polarization angle dependence is due to that for the present collision system, the laser field important is the projection along the internuclear axis. Figure 6 gives the Ne^+–He laser-induced charge transfer collision geometry. The impact velocity v is along the extraction field. The collision plane is defined by the impact parameter b and the projectile trajectory $R(t)$. α is the angle between the laser polarization and the collision plane.

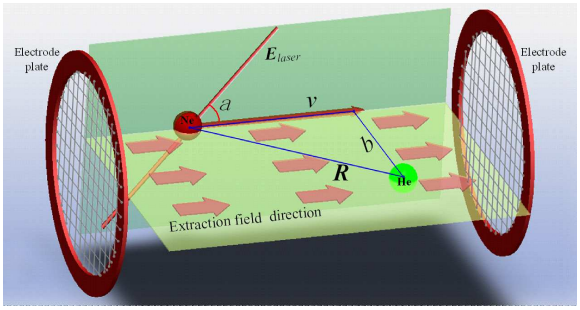

Fig. 6. Laser-induced Ne^+–He charge transfer collision geometry.

Since the internuclear axis rotates with respect to the lab-fixed laser polarization, the relevant electric field projection is thus

$$E(t) = E_0 \cos(\alpha)\nu t/R.$$

This expression does explain the polarization angle dependence in Fig. 6, which suggests that the enhancement does indeed vanish at $\alpha = \pi/2$ and $3\pi/2$.

When the laser wavelength is 410.16 nm and the collisional energy is equal to $E_p = 3.36 \times 10^{-6}$ keV/amu, the peak cross-section as a function of transfer laser intensity for the Ne^+–He system is given in Fig. 7. The collision cross-section rises with laser intensity and tends to saturate and there is a maximum cross-section of 3.2×10^{-17} cm^2 with the laser intensity of 1.1×10^{15} W/cm^2 in our results. When the collisional energy increases to 2.02×10^{-3} keV/amu, the situation is dramatically changed. The collisional coupling tends to play a dominant role in this region and the profile becomes a broad flat (see Fig. 7b).

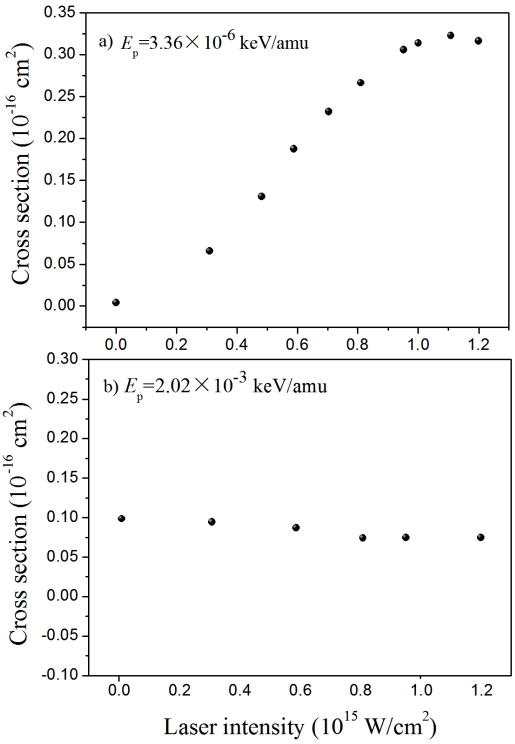

Fig. 7. Charge-transfer cross-section as a function of the transfer laser field intensity at different impact energy for Ne^+–He system.

3. Conclusion

In the present study, electron capture in slow asymmetric ion–atom collision system is considerably modified when the collision is embedded in a non-resonant laser field. Although the ionization potential of the Ne (21.6 eV) is less than He (24.6 eV), such a reaction is motivated by the anticipated use of strong laser field to modify energy flow pathway. In the low collisional energy region, the cross-section can be $\approx 10^{-17}$ cm^2 which is about two orders of magnitude higher than the collision-only process. With the increase of the collisional energy, the charge transfer cross-section for the Ne^+–He system in the presence and absence of a laser field tends to be equal. The two kinds of couplings of laser field and collision are of equal importance only in the small crossover region, where the charge-transfer cross-section shows an interference effect between the two mechanisms. Moreover,

the charge-transfer transition takes place in a much wider region than just around the "resonance point". Such result indicates that we can realize the interparticle charge transfer in a wide detuning range. The strong variation of the charge transfer cross-section with laser polarizations is studied. The capture probability in laser-assisted atom-ion collision varies significantly with the laser polarization angle. In our calculation we focus on parameters more favorable to experiment increasing our optimism that such an experiment can be done. The dependence of the charge transfer cross-section on the laser polarization has been confirmed and is in coincidence with previous experiment results [19]. The other calculation characteristics hold promise for being observable and have guiding significance for the further experimental work in the short future.

Acknowledgments

This work is supported by the National Natural Science Foundation of China (Grant No. 11304240 and 61378079) and the Fundamental Research Funds for the Central Universities.

References

[1] Y.P. Hsu, M. Kimura, R.E. Olson, *Phys. Rev. A* **31**, 576 (1985).

[2] Z.Z. Lu, Y.L. Sun, L. Ma, J.F. Liu, *Acta Phys. Pol. A* **127**, 1620 (2015).

[3] A. Gallagher, T. Holstein, *Phys. Rev. A* **16**, 2413 (1977).

[4] Z.Z. Lu, Y.L. Sun, L. Ma, J.F. Liu, *J. Phys. Chem. A* **119**, 1957 (2015).

[5] A. Agresti, P.R. Berman, A. Bambini, A. Stefanel, *Phys. Rev. A* **38**, 2259 (1988).

[6] S. Geltman, *Phys. Rev. A* **45**, 4792 (1992).

[7] A. Bambini, S. Geltman, *Phys. Rev. A* **50**, 5081 (1994).

[8] W.R. Green, M.D. Wright, J.F. Young, S.E. Harris, *Phys. Rev. Lett.* **43**, 120 (1979).

[9] Z.Z. Lu, D.Y. Chen, R.W. Fan, Y.Q. Xia, *Phys. Rev. A* **85**, 063402 (2012).

[10] L.B. Madsen, J.P. Hansen, L. Kocbach, *Phys. Rev. Lett.* **89**, 093202 (2002).

[11] M.F. Ciappina, *J. Phys. B At. Mol. Opt. Phys.* **40**, 4155 (2007).

[12] T. Kirchner, *Phys. Rev. Lett.* **89**, 093203 (2002).

[13] T. Kirchner, *Phys. Rev. A* **69**, 063412 (2004).

[14] L.F. Menchero, T. Kirchner, H.J. Ludde, *Phys. Rev. A* **79**, 023416 (2009).

[15] G.P. Harnwell, *Phys. Rev.* **29**, 683 (1927).

[16] F. Anis, V. Roudnev, R.C. Trujillo, B.D. Esry, *Phys. Rev. A* **73**, 043414 (2006).

[17] T. Kirchner, *Phys. Rev. A* **75**, 025401 (2007).

[18] L.F. Errea, L. Mendez, A. Riera, *J. Chem. Phys.* **79**, 4221 (1983).

[19] Z.Z. Lu, D.Y. Chen, R.W. Fan, Y.Q. Xia, *Appl. Phys. Lett.* **100**, 014105 (2012).